

Elastic constants of a superionic α -AgI single crystal determined by Brillouin scattering

L. Börjesson and L. M. Torell

Department of Physics, Chalmers University of Technology, S-412 96 Gothenburg, Sweden

(Received 11 March 1987)

For the first time Brillouin scattering experiments on single-crystal α -AgI have been performed. The spectra reveal all three acoustic modes of a cubic crystal, without any observable damping of the transverse modes in contrast to neutron scattering observations. The elastic constants were determined by fitting the observed Brillouin frequency shifts to the solutions of the dynamical equations for a cubic crystal of arbitrary but known orientation; the orientation relative to the light scattering configuration was established by transmission Laue x-ray diffraction. The obtained elastic constants, $C_{11}=1.48$, $C_{12}=1.29$, and $C_{44}=0.63$ in 10^{10} N m^{-2} , are noticeably small compared to those of low-conductivity β -AgI. The results reflect the disordered structure of α -AgI and are typical values of superionic conductors. The value of C_{44} is similar to those of other Ag^+ -conducting systems, i.e., AgCl and AgBr, while $C_{11}-C_{12}$ is much smaller for α -AgI, in support of a suggested structure-related model to explain the high conductivity. Indications of a structural transition were found in a temperature range around 640 K, i.e., in the range of a proposed cationic order-disorder transition. This is demonstrated by the behavior of the longitudinal mode, which rapidly decreased in frequency, accompanied with increased intensity and increased linewidth in the proposed transition range.

I. INTRODUCTION

Ionic conduction is well known in crystalline solids (for a review, see Ref. 1), and both cations and anions can carry current in certain circumstances. The materials are called superionic (or solid electrolytes) if the conductivity is comparable to that of liquid electrolytes ($\sim 10^{-1}-10^{-4}$ $\Omega^{-1}\text{cm}^{-1}$). Such a high ionic conduction may either be of the "point-defect" or the "molten-sublattice" type of mechanism. In the former, transport is through thermally generated Frenkel or Schottky defect pairs and conduction is therefore thermally activated; in the latter the number of ions of a particular type is less than the number of available sites in their sublattice and therefore a large number of ions are able to conduct with lower activation energy than for the defect process. Among the superionic conductors α -AgI has been the most extensively studied (for a review, see Ref. 2). It is regarded as the archetype of cationic conductors of the molten-sublattice type with an excellent conductivity³ and it is often used as the model substance in theories of solid electrolytes.^{4,5} The present study is devoted to a single-crystal Brillouin scattering study of α -AgI to investigate its elastic properties and determine the elastic constants.

So far, there are no reported data of measured elastic constants of α -AgI in the literature. Therefore, in theoretical models, either extrapolated values from a lower-temperature phase (γ -AgI)⁶ or estimated values from other Ag halide systems⁵ have been used in the calculations. An experimental determination of the elastic constants requires single crystals, which normally are cut, polished, and oriented at room temperature before

measurements. Lacking data for α -AgI is therefore probably due to experimental difficulties; in the case of α -AgI the crystals have to be grown and oriented at elevated temperatures, since the superionic phase exists in the temperature range 420–828 K, and the high-conductivity phase cannot be reached from the lower-temperature phase without cracking the crystal. Furthermore, arbitrary but known crystal orientations have to be employed, since it is difficult to impose a direction on the crystal growth in a sample cell, which is necessary for higher-temperature measurements.

In the present study we describe a technique for determining the elastic properties from light scattering studies of arbitrarily grown high-temperature single crystals. The method has also been used for determinations of the elastic constants of another single-crystal solid electrolyte, namely fcc- Li_2SO_4 .⁷ It is based on the Brillouin scattering technique. The data-analyzing method is that adapted by Stoicheff and coworkers in their studies of low-temperature rare-gas single crystals.⁸

AgI undergoes a first-order transition from a normal ionic conducting phase (β -AgI, wurtzite) into a highly conducting phase (α -AgI, cubic) at 420 K (see Table I for α -AgI data). At the transition the ionic conductivity increases abruptly four orders of magnitude to 1.3 $\Omega^{-1}\text{cm}^{-1}$ and thereafter there is a smooth increase to the maximum value of 2.6 $\Omega^{-1}\text{cm}^{-1}$ at the melting point at 828 K. Then, in the melting process, the ionic conductivity decreases, which is a peculiarity of AgI. The conducting phase is body-centered cubic (O_h^9-Im3m),⁹ with two iodine ions at the corners and body-centered position, and the two silver ions are randomly distributed over the 12 d sites of tetrahedral

TABLE I. Physical constants of α -AgI.

Molecular weight (g)	232.8
Transition temperature (K) ^a	420
Melting temperature (K) ^a	828
Density of 613 K (10^3 kg m^{-3})	5.89
Lattice constant at 573 K (\AA) ^b	5.089
Refractive index (at 613 K and 6471 \AA)	2.33

^aReference 37.^bReference 35.

iodine coordination¹⁰⁻¹² (which is also the coordination in the low-temperature wurtzite phase, see Fig. 1). Thus each Ag^+ has six equivalent sites available. Motions between these sites occur via the 24 h trigonal sites while the octahedral 6 b sites are empty.^{13,14} The large amount of available sites and the open structure may well explain the low activation energy ($\sim 0.1 \text{ eV}$) (Ref. 15) and the unusual conductivity characterizing this highly disordered phase.

The transition of the low-conductivity β phase into the high-conductivity α phase has been discussed in the terms of lattice forces, where decreasing values of the elastic constants play an important role. It has been argued that AgI in its β phase has an ionicity that is very near the stability limit.^{16,17} As the transition from the covalent bonding of the β phase to the ionic bonding of the α phase is approached, the elastic constant $(C_{11} - C_{12})/2$ approaches zero, indicating a lattice instability owing to vanishing of the bending force constant.^{17,18} The hexagonal iodine sublattice of the β phase can be transformed into a slightly deformed bcc lattice of the α phase by a low-lying optical mode observed by inelastic neutron scattering.¹⁸ This is because only a small amount of energy is required in the reorgan-

ization of the iodine sublattice, since the bending force constant of the β phase is very small. Recently, it has been shown that interaction potentials of the long-range Coulomb type, with integer ionic charges and which exhibit very strong van der Waals interaction, explain well the observed small elastic constant C_{44} in other silver halide systems (AgCl) and AgBr,¹⁹ as well as the violation ($C_{44} \neq C_{12}$) of the Cauchy relation. A small value of the elastic shear constant C_{44} generally leads to a low value of the activation energy for defect motion. This is therefore suggested to give an important contribution to the high ionic conductivity, observed in the silver halide systems.^{20,21} In other superionic materials, a dramatic softening of the elastic constant C_{11} has been found as the phase transition is approached,²²⁻²⁴ which has been related to the dynamic disorder and the melting sublattice of mobile ions of the high-conductivity phase. From the above it is clear that there are many reasons and a considerable interest in accurately determined elastic constants of α -AgI.

Much attention has been focused on the dynamics of the Ag ions in α -AgI^{6,10-14,25} and their interactions with the rigid iodide "cage."^{4,5} The hydrodynamics of the liquidlike Ag^+ sublattice has been predicted using a model of a crystalline cage immersed in a viscous liquid. From the absence of transverse modes in a Brillouin scattering study of α -AgI by Sasaki *et al.*,²⁶ it has been argued that there is a strong interaction between diffusing Ag ions and acoustic transverse phonons. Contrary we have previously demonstrated the existence of transverse acoustic phonons in Brillouin spectra of unoriented α -AgI single crystals.²⁷ These observations were obtained at a temperature of 563 K. However, there are several experimental indications of a subsequent order-disorder transition of the cation sublattice occurring at higher temperatures ($\sim 670-700 \text{ K}$).²⁸⁻³¹ One of the aims of the present study is therefore to obtain Brillouin spectra across the predicted transition. Apart from being used in the determinations of the elastic constants, the spectra will then by themselves reveal any anomaly in the longitudinal and the transverse modes as well as in the phonon propagation at the predicted transition temperature.

II. EXPERIMENTAL METHOD

In a Brillouin-scattering determination of the elastic constants of α -AgI, the major difficulties are the requirement of single crystals, grown and kept at high temperatures, as well as the necessity of using a high-resolution light scattering technique. The method used to grow and orient high-temperature single crystals and the Brillouin equipment employed is described below.

A. Single-crystal preparation and x-ray apparatus

In a conventional Brillouin-scattering experiment for determining the elastic constants of a crystal, the scattering wave vector \mathbf{q} is directed along a high-symmetry direction of the crystal. This was not possible due to experimental difficulties in case of α -AgI since it only exists at elevated temperatures 420–828 K and sin-

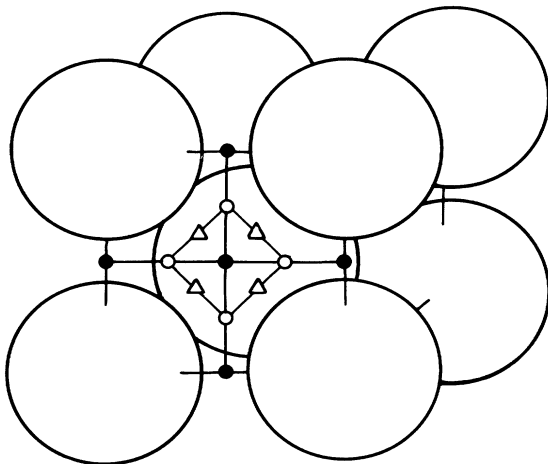


FIG. 1. High temperature α phase of AgI. Large circles represent the I^- bcc lattice. Possible sites of Ag^+ are shown on the front face for the 6 b (closed circles) sites, for the 12 d (open circles) sites, and for the 24 h (open triangles) sites.

gle crystals of α -AgI have to be grown from the melt. Passing a β -AgI single crystal, grown at room temperature, through the first-order β - α phase transition at 147°C results, unfortunately, in crystal cracking due to large volume changes at the transition. The crystals were therefore grown in sample cells, cylindrical in shape, in which it was difficult to impose a direction on the crystal growth. Since the scattering vector is fixed by the experimental geometry, the orientation of the crystal must be determined relative to the laboratory reference frame. This was accomplished by x-ray diffraction. The Brillouin-scattering experiment is then performed with a scattering vector in an arbitrary but known crystal direction. A fitting procedure, described in Sec. III, therefore had to be used to determine the elastic constants from the Brillouin frequency shifts and the crystal orientation.

The furnace was especially designed for growing single crystals and performing Brillouin-scattering studies and, at the same time, allowed x-ray analyses to be made. The position of the furnace and the geometry of the scattering experiment is shown in Fig. 2 and a cross section of the furnace can be seen in Fig. 3. It is made of two ceramic tubes which fitted into each other. The diameter of the inner tube is 10 mm and a track is ground on the outside in order to support the heating coil. The space between the outer tube and the water-cooled brass mantle is filled with insulating material. The furnace was constructed with several openings. The conical opening (outer diameter 25 mm) situated on the cylindrical wall permits x-ray analysis of the crystal. The diameter is a compromise between, on one hand, a large opening allowing many Laue diffraction spots for easy determination of crystal orientation and, on the other hand, a small opening to prevent unnecessary heat loss. Opposite to the conical opening is a 5-mm-diameter port for the entrance of the collimated x-ray beam. The collimator defines the reference axis of the x-ray apparatus as well as that of the light scattering apparatus and the optical system was aligned with a laser beam that passed through the collimator. This is essential since the reference axis is the link between the Laue photos and the Brillouin spectra. The light port of the incident laser beam, at the bottom of the furnace, is closed by an

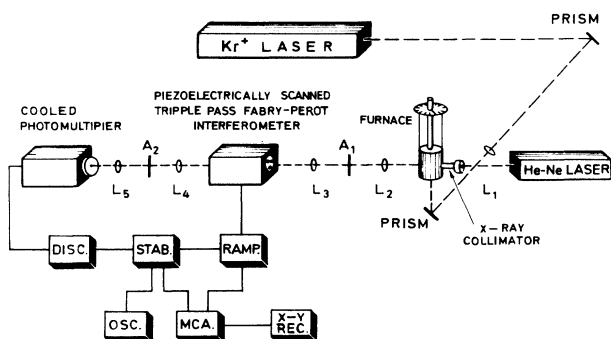


FIG. 2. Brillouin-scattering apparatus.

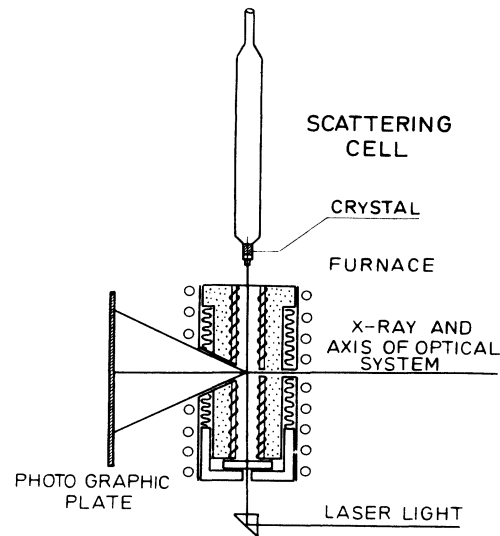


FIG. 3. Scattering cell and cross section of the furnace.

optical-flat fused-silica window. The scattered light is collected at an angle of 90° by using the conical opening, which is then partially closed by a metal disc with only a 4-mm-diameter opening to reduce unnecessary heat losses during the Brillouin-scattering experiments. A cell holder is placed on top of the furnace and it consists of a rotatable brass tube with a pointer that indicates the angular position of the cell on a 360° scale. The accuracy of the pointer is about $\pm 0.3^\circ$. Rotations of the sample cell permit Brillouin spectra to be obtained for different crystal orientations, a capability essential for the determination of the elastic constants.

The temperature was measured by a calibrated thermocouple attached to the upper part of the crystal inside the sample cell. The temperature stability at the scattering point was better than ± 2 K during a measurement running for several hours. The temperature gradient in the middle part of the furnace, caused mainly by the conical opening, was checked by measuring the temperature at different points along the vertical axis inside the furnace over a distance of 15 mm at the melting temperature of AgI (828 K). It was found to be about 10 K with the metal disc covering the conical opening and 15 K without the metal disc. This temperature gradient was in fact used for the growth of the crystal, see below.

Sample cells were made of Vycor tubes of two different sizes; one with a 9 mm diameter, the other with an inner diameter of either 2 or 3 mm, see Fig. 3. A quartz window of the same size as the inner diameter of the thin tube was used as a light port for the incident light at the bottom of the cell. The 9 mm diameter tube was sufficiently long, ≈ 200 mm, to be rotated from the outside of the furnace which allows different angular settings of the crystal. The 2 mm (or alternatively 3 mm) diameter tube, 15 mm long, constituted the scattering cell. The sample cells were carefully cleaned with ultrasonic equipment, which was essential both for the

single-crystal growth and for reducing parasitic scattering. The sample cell was filled with a 1-mm layer of powder AgI (Riedel de Haen). Then the temperature was raised to just above the melting point. After cooling to about 800 K more powder was filled and melted again. This procedure was necessary in order to avoid air bubbles in the crystal and it was repeated until a clear melt of approximately 5–6 mm height was obtained. The crystal was grown by a modified Bridgman technique, i.e., by moving the molten material in a temperature gradient. Then the gradient caused by the conical opening in the furnace was used. Hence, when a crystal was grown, the temperature at the center of the furnace was about 823 K and 15 mm above it was about 838 K. The cell was placed 15 mm above the center and lowered with a speed of 5 mm per hour into the central part of the furnace. The grown crystals were cylindrical in shape, 2 or 3 mm in diameter, 5–6 mm long, and of good optical quality. The color of the crystals was red near the melting point and it gradually changed to pale yellow when decreasing the temperature to near the α - β transition.

The orientation of the crystal relative to the light scattering geometry, as well as the single crystal quality of the sample, were determined by means of the transmission Laue x-ray diffraction method. A standard Philips x-ray equipment with a tungsten tube operating at 60 kV and 16 mA was used. The diffraction pattern was recorded on a Polaroid type-57 film held in a Polaroid XR-7 cassette. The distance between the crystal and the film was 75 mm. To ensure that the collimator was directed to the center of the film, a second collimator was used and held in a track adapter fitting the Philips x-ray equipment. The collimator was also used to align the optical system since its axis coincided with the axis of the Brillouin-scattering optics.

Two single crystals were grown for light scattering studies. Due to the large x-ray absorption of AgI no diffraction spots were obtained for the larger crystal, i.e., crystal 1 of diameter 3 mm, despite very long exposure time and trials with different rotation angles. However, for crystal 2, which had a smaller diameter of 2 mm, five Laue photographs taken at five different rotation angles (in steps of 10°) showed 5–8 distinct diffraction spots. These photographs were analyzed to yield the orientation of the crystal axis with respect to the laboratory reference frame. The orientation is expressed in terms of the Euler angles (Ψ , Θ , Φ) as defined by Goldstein.³² An advantage of choosing the Euler angles is that when rotating the sample cell for different crystal settings, only one angle is changed, namely Φ , the others being fixed. The Euler angles, calculated from the different Laue photographs, are presented in Table II. The uncertainties in the determination of the angles were estimated to be $\pm 2^\circ$, which include the effect of a slight precession of the cell upon rotation.

B. Brillouin apparatus

A schematic diagram of the experimental equipment is shown in Fig. 2. As a light source the emission at 568.2 and 647.1 nm from a Spectra Physics model 165-00

TABLE II. Crystal orientation as specified by the Euler angles for two AgI single crystals. In case of crystal 1 Φ_{rot} specifies the angles at which Laue photographs were taken.

Crystal	Φ_{rot} (deg)	Ψ (deg)	Θ (deg)	Φ (deg)
1	0	-1.7	28.7	-2.4
2	340	-18.0	29.0	129.0
	350	-19.5	29.0	120.5
	0	-19.2	28.5	109
	10	-18.5	30.0	99
	20	-17.5	31.0	87.5

krypton laser was used. Red light is necessary in a temperature study of α -AgI since the color of the crystal change from being yellow just above the transition temperature to dark red close to the melting point. The laser output power was reduced to approximately 200 mW for all measurements to minimize photoreduction of Ag in the sample. The laser was operating in a single-frequency mode by using a thermally stabilized etalon in the cavity. Stabilization was essential since in some cases accumulation times of the spectra of several hours were necessary and thermal mode drifts would cause unacceptable loss in resolution. The laser light was incident along the vertical axis of the sample cell and scattered light at an angle of 90° was analyzed by a Fabry-Perot interferometer (Burleigh model RC-110).

In the present study, triple passing of the Fabry-Perot interferometer was used in order to resolve the transverse modes in the Brillouin spectra, which otherwise are totally obscured by the large Rayleigh peak, for a typical spectra see Fig. 4. This is a general problem for light scattering measurements in solids, i.e., an intense Rayleigh peak close to weak Brillouin peaks, and a way to increase the contrast of the signals is to use multipass interferometry. Moreover, multipassing increases the instrumental resolution (by a factor of two for triple passing), which is related to the finesse F of the Fabry-Perot spectrometer. Other factors which influence the finesse are the mirror flatness and parallelism, the mirror

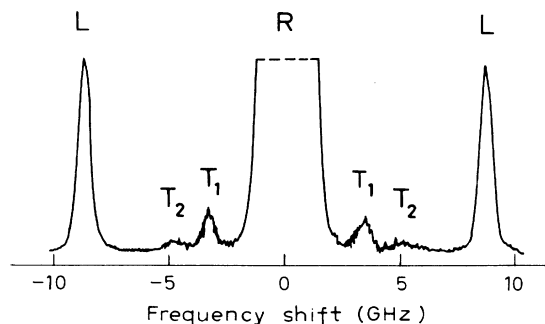


FIG. 4. Brillouin spectrum of α -AgI at 613 K; R, L, and T are Rayleigh, longitudinal-Brillouin, and transverse-Brillouin components, respectively.

reflectivity, and the size of the pinhole aperture A_2 . For an optimum combination of resolution and light gathering power, the latter three contributions to the instrumental function should be equal. In the present study a 200- μm pinhole was used, the mirrors were flat to $\lambda/200$ and dielectrically coated for a reflectivity of 93% and 600 nm. The value of the reflectivity was chosen to fit the triple-pass unit. The measured total instrumental finesse for the triple-pass system was above 30 for all measurements. The interferometer was stabilized for frequency drift of the laser and cavity drift of the interferometer (cavity stabilization) as well as for parallelism of the interferometer mirrors (finesse stabilization). Three different mirror settings were used corresponding to free spectral range of 25.46, 16.78, and 15.14 GHz, respectively; 25.46 GHz was chosen to record the longitudinal mode and the other settings to resolve the transverse modes.

The detection system consisted of a cooled ITT-FW-130 photomultiplier tube and photon-counting electronics with a dark current of less than five counts per second. The signal was stored in a multichannel analyzer (Tracor Northern 1705).

The spectrometer axis was defined by directing a He-Ne laser beam (see Fig. 2) through the x-ray collimator and using the beam for correct setting of lenses and apertures. This axis defined the y axis of the laboratory reference frame. The exciting Kr^+ laser beam was then aligned to intersect the y axis at the scattering point at an angle of 90° , i.e., parallel to the z axis of the laboratory coordinate system.

III. DATA ANALYSIS METHOD

The elastic constants, which in the case of a cubic crystal are given by the three independent constants C_{11} , C_{12} , and C_{44} , were obtained from the measured Brillouin frequency shifts. The calculations are based on the theory for scattering of light from thermally excited sound waves in cubic crystals presented by Benedek and Fritsch.³³ The method, summarized below, is essentially the same as that used by Stoicheff and coworkers in their light scattering study at low temperatures on rare-gas single crystals.⁸

It is the fluctuations in the dielectric constants of a medium which give rise to scattered light. In Brillouin scattering these fluctuations are due to thermally excited propagating elastic waves, which can be represented by the equation

$$u_j = u_{0j} \exp[i(\mathbf{q} \cdot \mathbf{r} - \omega t)] \quad (1)$$

describing plane and monochromatic waves. The acoustic wave vector \mathbf{q} is then related to the wave vectors of the incident and the scattered light, \mathbf{k}_i and \mathbf{k}_s , respectively, according to

$$\mathbf{q} = \pm(\mathbf{k}_i - \mathbf{k}_s) \quad (2)$$

The frequency $\omega(\mathbf{q})$ of the acoustic mode responsible for the scattered light is equal to the experimentally measured Brillouin shift Ω , for which the usual Brillouin equation holds, i.e.,

$$\Omega = \pm 2n \frac{v(\hat{\mathbf{q}})}{\lambda_0} \sin(\alpha/2) \quad (3)$$

which relates the frequency shifts of the scattered light Ω to the acoustic velocity $v(\hat{\mathbf{q}}) = \omega(\mathbf{q})/|\mathbf{q}|$. In Eq. (3) n is the refractive index of the crystal, λ_0 is the wavelength of the incident light in vacuo, and α is the scattering angle. For an adiabatic propagation of the acoustic wave the equations of motion can be written

$$(\lambda_{ij} - \rho\omega^2\delta_{ij})u_{0j} = 0, \quad (4)$$

where δ_{ij} is the Kronecker δ function, ρ is the density of the crystal, and λ_{ij} are given by

$$\lambda_{ij} = (C_{11} - C_{44})q_i^2 + C_{44}q^2 \quad (i=j), \quad (5)$$

$$\lambda_{ij} = (C_{12} + C_{44})q_i q_j \quad (i \neq j). \quad (6)$$

q_i are the components of the acoustic wave vector \mathbf{q} in the crystal reference frame with

$$q^2 = \sum_{i=1}^3 q_i^2. \quad (7)$$

The relationship between the adiabatic elastic constants of the crystal and the frequency shifts in the Brillouin spectrum is then given by the secular equation

$$|\lambda_{ij} - \rho\Omega^2\delta_{ij}| = 0 \quad (8)$$

with three positive roots $\Omega_\mu(q)$, $\mu=1, 2$, and 3 , corresponding to the two transverse modes T_1 and T_2 and the longitudinal mode L , respectively. It should be noted that it is only in the high-symmetry directions $\langle 100 \rangle$, $\langle 110 \rangle$, and $\langle 111 \rangle$ that the modes can be described as purely transverse or longitudinal; in all other directions the polarization is mixed, however, being either predominantly longitudinal or transverse.

From the equations given above, it is obvious that for known components of \mathbf{q} in the crystal reference frame, and for known elastic constants the Brillouin shifts can be determined directly. However, it is the inverse problem which must be solved; from experimentally measured Brillouin shifts the elastic constants should be determined. In general it is not practical to solve the equation in closed form because of the necessity to invert the diagonalization of λ_{ij} . This can be done for the special case when \mathbf{q} is parallel to one of the principal symmetry directions. In the present work, however, it was not possible to orient the crystal according to the laboratory reference frame. For a correct calculation of the elastic constants, Eq. (8), i.e., the 3×3 eigenvalue problem, has to be solved. This was accomplished by a computer program using a least-squares fitting routine, starting with a set of trial values of the elastic constants, which were then adjusted in order to obtain the best agreement between the calculated and observed Brillouin shifts.³⁴

IV. EXPERIMENTAL RESULTS

A. Brillouin spectra

Two α -AgI single crystals were investigated by Brillouin scattering and a typical spectrum, obtained at 613

K, is reproduced in Fig. 4. The figure shows all three Brillouin components as expected from a cubic crystal; a strong longitudinal mode (L) and two transverse components (T_1 and T_2) of considerably weaker intensity. Both crystals were observed in a range of crystal orientations by rotating the sample around the vertical axis of the sample cell, see Fig. 3. In total 102 spectra were obtained. The longitudinal component was present in all recordings, the T_1 mode in all but four of the spectra, and the T_2 mode only in 27 spectra. The intensities of the different components depend on crystal orientation and on temperature, see Sec. V.

Spectra were recorded for a full rotation of 360° at about 10° intervals. The measured frequency shifts of the Brillouin components are shown in Figs. 5(a) and 5(b) for crystals 1 and 2 obtained at a temperature of 563 and 613 K, respectively. Large variations in the frequency shifts with crystal orientation are observed which indicate that the single-crystal samples are characterized by a high degree of elastic anisotropy. The temperature dependence of the frequency shifts was obtained in the range 455–789 K from crystal 2 for two different crystal orientations specified by an Euler angle of Φ of 128° and 19° , respectively. Results for the longitudinal and the transverse T_1 frequency shifts are shown in Fig. 6. A dramatic change at about 640 K in the linear (within the

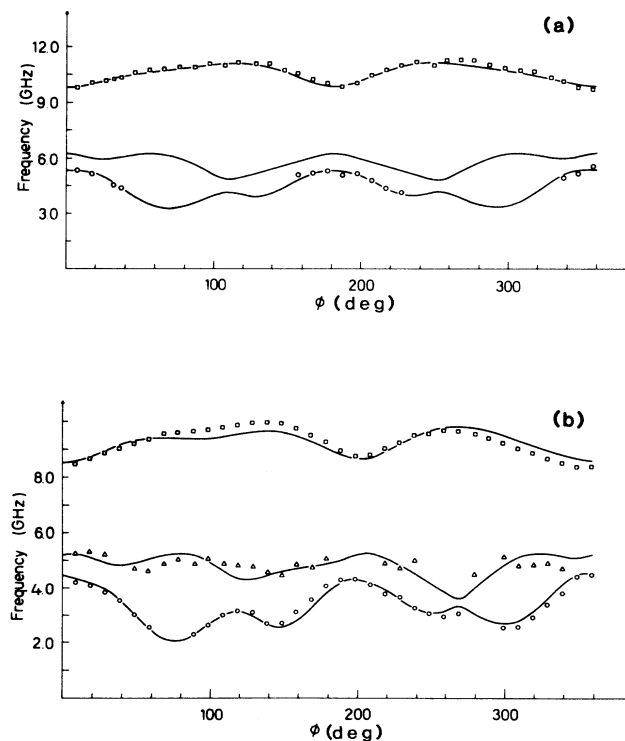


FIG. 5. Observed Brillouin shifts of α -AgI vs rotation angle Φ for (a) crystal 1 at 563 K and (b) crystal 2 at 613 K. Longitudinal shifts are represented by \square , transverse T_1 by \circ , and transverse T_2 by \triangle . Solid lines represent calculated fits from the determined values of the elastic constants.

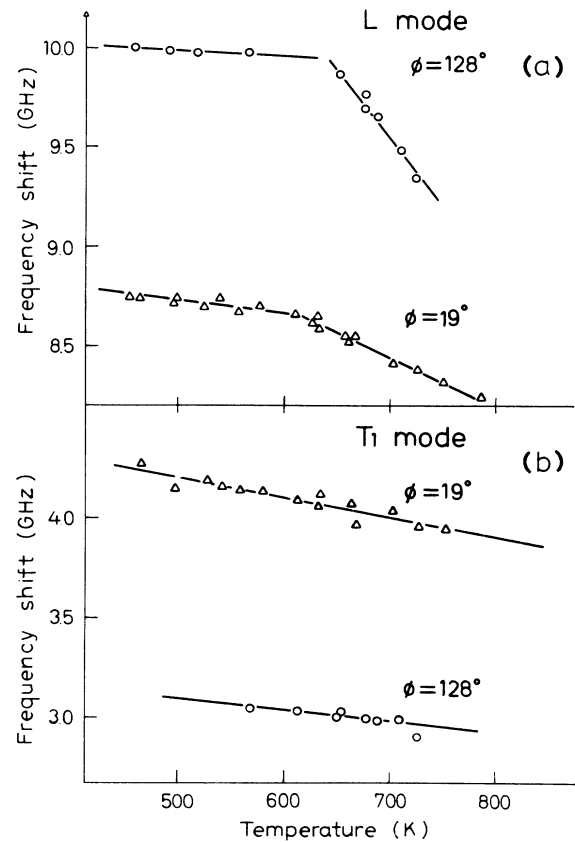


FIG. 6. Temperature dependence of the acoustic mode frequencies in α -AgI at two different crystal orientations represented by Euler angles (Ψ , Θ , Φ) of $(-18.5^\circ, 29.5^\circ, 128^\circ)$ and $(-18.5^\circ, 29.5^\circ, 19^\circ)$, respectively. Longitudinal shifts are shown in (a) and transverse T_1 shifts in (b).

experimental error) temperature coefficient of the longitudinal frequency shift is recorded. No such effect is observed in case of the transverse frequency shift.

Each frequency shift is the average of at least 5000 sweeps during a scanning time of about 20 minutes. However, the recordings of the weak transverse modes often required longer scanning times which therefore in some cases were extended to about two hours. The inaccuracy of the measurements of the frequency shifts varied from about 1% for the most intense components to about 5% for the weakest transverse modes.

B. Elastic constants

For a given set of trial values of the elastic constants, the frequencies of the acoustic modes were calculated from Eq. (8) for all orientations of the crystal at which Brillouin spectra have been recorded. The calculated values of the acoustic-mode frequencies were compared to the corresponding experimental frequency shifts and a fit was obtained for each crystal by the method of minimizing the sum of the squares. In these calculations a value of the refractive index was needed. There is, to our knowledge, no data in the literature of the refractive

index of bcc-AgI which therefore was measured in our laboratory. A thermo-optical method was used which is based on interferometry and which has been described previously.³⁵⁻³⁸ The result for $\lambda=6471 \text{ \AA}$ and $T=613 \text{ K}$ is presented in Table I. A slight wavelength dependence was observed in the yellow-red wavelength range at the temperatures of the present study; the refractive index being about 2.34 for the wavelength 568.2 nm used in the study of crystal 1 at a temperature of 563 K.

Density data were obtained from structure parameters,¹⁴ which resulted in a temperature dependence of $0.58 \text{ kg m}^{-3} \text{ K}^{-1}$ in the range of interest. The calculated value at 613 K is presented in Table I. Other input data needed are the components q [see Eqs. (5) and (6)] which were obtained in the reference frame of the crystal by using the Euler angles. The latter could be calculated for crystal 2 for which the crystal orientation was established by x-ray diffraction (see corresponding Euler angles of Table II). Table III summarizes the results of the elastic constants obtained for crystal 2 by using Brillouin data for all observed crystal orientations. The resulting frequency fit from the minimizing procedure is shown in Fig. 5(b), where solid lines represent the theoretical value based on the elastic constants of Table III. Close agreement is obtained for all crystal orientations. The absolute values of the elastic constants are estimated to be accurate to better than 4% considering uncertainties in scattering angle, temperature, density, and refractive index as well as the errors in the determination of the Brillouin shifts and the Euler angles.⁷

In case of crystal 1, i.e., the larger crystal, the orientation could not be determined by the Laue technique due to the large x-ray absorption of the crystal. Therefore, in these calculations not only the elastic constants but also the Euler angles were used as free parameters in the minimizing procedure. These calculations were therefore interesting in themselves since they served as a test of the reliability of the Brillouin technique as a possible method for determining elastic properties of unoriented crystals. The results of such calculations are $C_{11}=1.5$, $C_{12}=1.1$, and $C_{44}=0.7$ expressed in 10^{10} N m^{-2} . These results correspond within 1% in case of C_{11} , 6% for C_{44} , and 13% in case of C_{12} , to the results of crystal 2, for which the orientation is known. The larger uncertainties of the C_{12} values are explained by the weak intensities of the transverse modes. The results imply that unoriented crystals can readily be used provided there

are enough measurements obtained at different crystal orientations. The resulting Euler angles of crystal 1 are shown in Table II.

Several quantities directly related to the elastic constants were calculated: The bulk modulus $B = (\frac{1}{3})(C_{11} + 2C_{12})$, the elastic anisotropy $A = 2C_{44} / (C_{11} - C_{12})$, and the velocities of sound in high symmetry directions.³⁶ The results are given in Tables III and IV.

V. DISCUSSION

A. Transverse mode

Without any further analyses of the Brillouin data obtained on α -AgI, the spectra in themselves explain several aspects discussed in theories of solid electrolytes, in which data of α -AgI often are used for numerical estimations of predicted behavior.^{4,5} The dynamics have been discussed in terms of an interaction between a charged liquid of mobile ions (Ag^+) and a rigid crystalline (I^-) cage. It has been proposed that this interaction causes the transverse phonons of the cage to couple via inertial forces to the viscous ion current and as a result damping of the transverse-acoustic modes should be observed. In fact, neutron scattering studies of single crystal α -AgI (Ref. 39) report an extremely large linewidth observed for the transverse-acoustic phonon modes at a frequency of about 18 cm^{-1} . Also, in Brillouin scattering from α -AgI the absence of transverse modes has been reported and interpreted as being due to a strong interaction between the diffusion motion of Ag^+ and the propagating transverse-acoustic wave.²⁶

The present study, however, reveals both the T_1 and T_2 transverse modes which were also observed in the preliminary study of unoriented single crystal α -AgI of this laboratory.²⁷ The latter measurements were performed at a temperature of 563 K, i.e., below the temperature of a possible order-disorder-like transition which has experimentally been observed around 670 K as a singularity in the specific heat,²⁸ a change in the activation energy of the ionic conductivity,²⁹ and a decrease in the Raman intensity³⁰ as well as in molecular-dynamics simulation studies.³¹ It has been suggested that the Ag^+ sublattice retains some form of ordering upon transition from the β to the α phase, and that such residual Ag^+ sublattice vanishes in a temperature range about the temperature of the 670-K transition.²⁹⁻³¹ In this model liquidlike behavior of the Ag ions is only ex-

TABLE III. Elastic data on some silver halide crystals.

Material	Temperature (K)	Elastic constants (10^{10} N m^{-2})			Adiabatic bulk modulus (10^{10} N m^{-2})	Elastic anisotropy
		C_{11}	C_{12}	C_{44}		
AgI	613	1.48	1.29	0.63	1.35	6.63
AgBr ^a	623	3.63	2.55	0.8	2.91	1.48
AgCl ^b	295	5.86	3.58	0.62	4.34	0.54

^aReference 21.

^bReference 38.

TABLE IV. Velocities of sound (in m s^{-1}) in high symmetry directions of α -AgI at 613 K.

	Crystal directions		
	$\langle 100 \rangle$	$\langle 110 \rangle$	$\langle 111 \rangle$
v_L	1585	1849	1929
v_{T_1}	1034	402	681
v_{T_2}	1034	1034	681

pected above the transition range. Any coupling between a charged liquid and a rigid cage is therefore to be found at these higher temperatures. With this in mind, Brillouin spectra at different temperatures were recorded over the suggested transition range. Transverse modes were observed over the whole range. Moreover, no change (within the experimental accuracy) could be observed in neither the intensities nor in the temperature dependence of the frequency shifts of the transverse modes, see Fig. 6. We therefore conclude that no strong interaction is present between the Ag^+ diffusion and the transverse acoustic waves at GHz frequencies. The absence of transverse peaks in the previous Brillouin study of Sasaki *et al.*²⁶ is not very surprising since they use backscattering geometry, for which the transverse peaks are forbidden from the selection rules.

It is then to be noted that interactions between diffusive motions and sound waves have in fact recently been observed at the high frequencies of Brillouin scattering. The effect was demonstrated in this laboratory as internal-friction peaks in other fast-ion conducting systems due to motions of Ag^+ , namely in AgI-doped glasses.⁴⁰ In the latter systems the observed broadening of the Brillouin components reached its maximum value at a frequency given by the peak condition for absorption, i.e., $\omega\tau \approx 1$, where τ is the relaxation time due to diffusing Ag^+ as determined from conductivity data. In the present case of α -AgI the transition from the oscillatory motion to the diffusive motion of Ag^+ takes place in the frequency range 3–10 cm^{-1} (Ref. 39). Frequency-dependent conductivity measurements show high values for the conductivity down to 3 cm^{-1} (i.e., ≈ 90 GHz) which is more than an order of magnitude larger than the present probe frequency. Dampings at Brillouin frequencies are therefore to be sought at considerably lower temperatures, at which the conductivity is an order of magnitude smaller (i.e., τ is increased by the same factor). However, such low temperatures are outside the stability range of α -AgI. Interactions between diffusing Ag^+ and either the longitudinal or the transverse mode can therefore hardly be expected for α -AgI at Brillouin frequencies. In the neutron scattering study of Brüesch, Bührer, and Smeets,³⁹ however, the transverse mode was observed in the frequency range of high Ag^+ conductivity and consequently the corresponding linewidth was considerably damped.

B. Longitudinal mode and cationic phase transition

In the following paragraph the behavior of the longitudinal mode will be discussed. The temperature plot of the observed longitudinal frequency shift shows an interesting feature, see Fig. 6. Contrary to the observations for the transverse frequency shifts, there is a distinct change in the temperature coefficient in the range of the proposed order-disorder transition temperature around 670 K. Also, it can be seen in Fig. 6 that the temperature coefficient above the transition depends on the direction of propagation of the acoustic wave. It is interesting to note that this sudden change of temperature coefficient of the longitudinal shift is followed by an

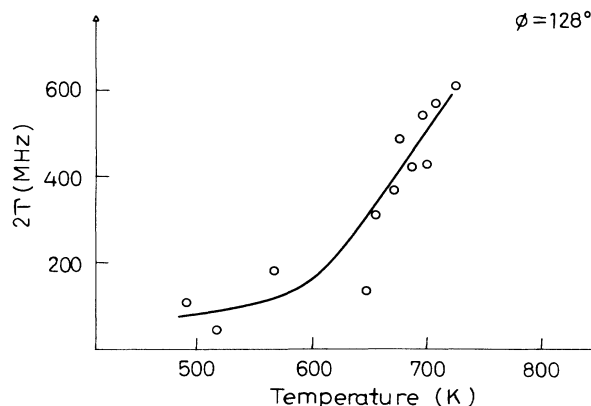


FIG. 7. Longitudinal Brillouin linewidth vs temperature in α -AgI for fixed Euler angles (Ψ , Θ , Φ) of $(-18.5^\circ, 29.5^\circ, 128^\circ)$.

increasing linewidth of the corresponding mode, see Fig. 7. The width was determined by subtracting the instrumental width, as measured from the central line, from the width of the observed Brillouin component. Moreover, in the same temperature range the intensity changed rapidly. In Fig. 8 the intensity ratio between the longitudinal and the transverse (T_1) mode is shown versus temperature for two different crystal orientations. The scattering of the data in Fig. 8 reflects mainly the inaccuracy in determining the intensities of the weak T_1 mode. However, a maximum of the intensity ratio is definitely observed and it is caused by an increasing and later decreasing intensity of the longitudinal mode. All three effects for the longitudinal mode discussed above, i.e., an intensity maximum followed by a change in temperature coefficient of the shifts and by an increasing linewidth, are effects typical of the behavior of the Brillouin component for a material when passing the glass

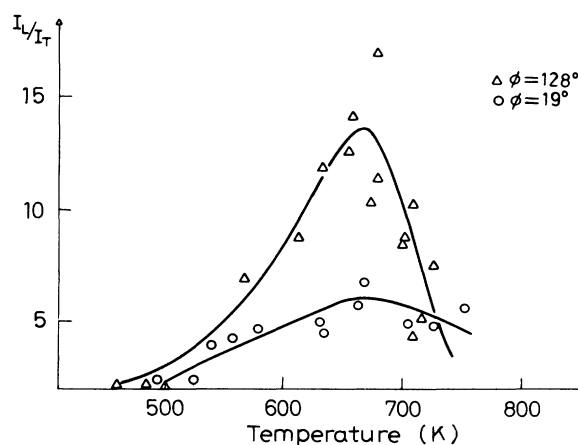


FIG. 8. Intensity ratio between longitudinal (L) and transverse (T_1) Brillouin mode in α -AgI vs temperature for two crystal orientations represented by Euler angles (Ψ , Θ , Φ) of $(-18.5^\circ, 29.5^\circ, 128^\circ)$ and $(-18.5^\circ, 29.5^\circ, 19^\circ)$, respectively.

transition. Since all the effects appear in the range for the predicted transition and are typical features at a melting process, we conclude that the origin is structural, in favor of a cation order-disorder transition.

Recently, a model for the distribution of the cations in α -AgI has been proposed from Raman scattering measurements. A high correlation between the silver ions are suggested at low temperatures, which creates local charge fluctuations and local anisotropy in the iodine polarizability. This correlation vanishes with increasing temperature. The Raman data indicate that the transition temperature occurs around 700 K. At higher temperatures the Ag^+ distribution becomes homogeneous and isotropic. Present intensity data confirm a change in the local polarizability around 700 K. The observed decrease in intensity at higher temperatures support the model of an isotropic distribution of Ag^+ in the lattice. The lifetime of the phonons, which couple to fluctuations in the local site populations of Ag^+ , has been estimated for α -AgI in the theory of Huberman and Martin.⁴ These fluctuations, the so-called pseudospin density fluctuations, can be divided into two categories: Local fluctuations due to ion redistribution among (1) energetically inequivalent sites (2) symmetry-energetically-equivalent sites. The former couple to pure volume strains and the latter only to shear strains. The present observation of a damping of the longitudinal wave are thus in favor of a redistribution of Ag^+ close to the transition temperature from jumping between equivalent (tetrahedral) to also include jumps to inequivalent (trigonal and octagonal) sites. This might then reflect the onset of an isotropic distribution as discussed by Fontana *et al.*^{29,30} It is also interesting to compare the expected broadening of acoustic phonons which couple to the pseudospin fluctuations of the charged liquid. Huberman and Martin predict, for a phonon frequency of 10^{10} Hz, a 6% broadening in case of α -AgI.⁴ This is in fact the maximum broadening as observed in the present study of the longitudinal mode, i.e., in the Ag^+ liquid range above the observed transition, see Fig. 7. The theory also predicts a much stronger damping due to pseudospin fluctuations than any damping due to coupling between transverse phonons and the viscous ion current; the relative magnitudes of the two processes were estimated to be $10^3:1$, respectively, in case of α -AgI. This implies a broadening of the transverse components of about $6 \times 10^{-3}\%$ which is far below the accuracy of the present measurements. Thus, the absence of any damping of the observed transverse components are also in accordance with the predictions of Huberman and Martin.⁴

C. Comparison of elastic constants

The obtained values for the elastic constants are small compared to those of normal, low-conducting ionic crystals.^{41,42} It is of special interest to relate present values of the high conducting α phase with corresponding elastic constants of the low-conducting wurtzite β -AgI. The latter have been measured by Fjeldly and Hansson,¹⁷ who also transformed the obtained room temperature

values to cubic elastic constants. These values are shown in Fig. 9 together with the resulting fits of the present study extrapolated to room temperature. The temperature dependences of the elastic constants of the α phase were obtained from the variations of the frequency shifts with temperatures shown in Fig. 6. Solid lines of Fig. 9 are results of such calculations, whereas dashed lines represent extrapolated values. Comparing these extrapolated α -AgI values with the corresponding transformed elastic constants of β -AgI at room temperature one finds that those of the α phase are considerably lower. The effect is especially pronounced in case of C_{11} and C_{12} , for which the values decrease to about half the room temperature values of β -AgI. The same phenomena have been observed in other superionic crystals, namely in fluorite solid electrolytes,^{22,23} in SrCl_2 (Ref. 24), and in AgBr ,²¹ for which the transition in the high conducting state is a smooth transition. In the latter systems it is the value of C_{11} which is subject to the largest changes at the transition from the low to the high conducting phase. Recently, another solid electrolyte has been studied in this laboratory, namely fcc- Li_2SO_4 , which is characterized by a first-order transition as is the β - α transition of AgI. Then it is not possible to make observations by light scattering while passing the transition since the single crystal is ruined by cracks and multidomains. However, again low elastic constants were obtained and a decrease of both the C_{11} and C_{12} values were observed when compared to the corresponding values of similar but nonconducting ionic crystals. The phenomenon seems to be a general characteristic of the solid electrolytes and reflects the soft disordered crystal structure typical for these materials.

It has been suggested that low elastic constants are essential for obtaining high ionic conductivity.^{20,21} For

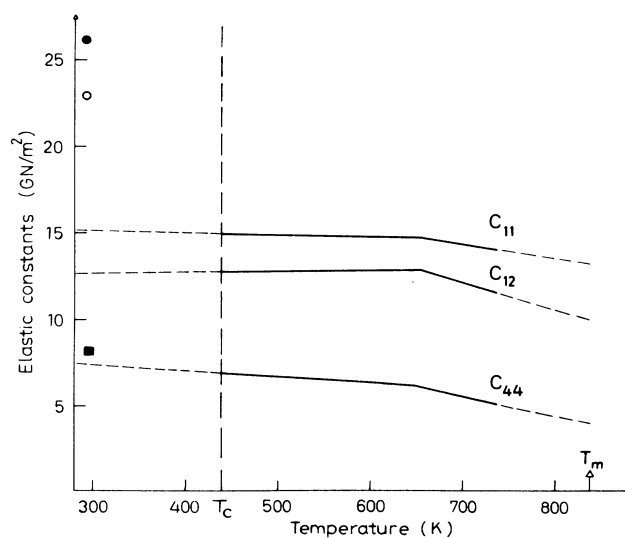


FIG. 9. Temperature dependence of the elastic constants. Solid lines represent present results for α -AgI; dashed lines are extrapolations. Room temperature values of C_{11} (●), C_{12} (○), and C_{44} (□) for β -AgI are from Ref. 17.

the silver halides AgCl and AgBr low values of the transverse optic phonon frequencies and of the elastic shear constant C_{44} have been explained by the quadrupolar deformability of the silver ions. It has been shown that this mechanism leads to a decrease of the activation energy for vacancy and interstitial diffusion and therefore contributes to the anomalously high conductivity of silver ions. The activation energy of the deformation of the surrounding halide sublattice due to diffusing Ag^+ is in this model related to the elastic constants according to

$$E \sim [(C_{11} - C_{12}) + 3C_{44}] . \quad (9)$$

The corresponding values of the elastic constants for AgBr and AgCl are shown in Table III. A comparison with the present values of α -AgI shows even lower values of $(C_{11} - C_{12})$ for α -AgI. This is also found when comparing the β and α phases of AgI for which both C_{44} and $(C_{11} - C_{12})$ decrease through the β - α transition. The decrease in the deformation activation energy may be an important contribution to the high conductivity of the α phase, even though the diffusion of Ag^+ in case of α -AgI occurs between empty available sites in a regular lattice rather than by interstitial and vacancy diffusion as in AgBr and AgCl.

In the high conducting α phase the temperature dependences of the elastic constants correspond to the normal linear decrease of the elastic stiffness with increasing temperature due to anharmonicity, for the temperature range just above the transition at 420 K. However, in the range of the suggested subsequent transition at ≈ 670 K a marked softening of the elastic constants is observed, see Fig. 9, which again indicates a structural change in support of a proposed cationic order-disorder transition. It is then to be noted that this is not only the

case for C_{11} but also for the shear elastic constants C_{44} and $\frac{1}{2}(C_{11} - C_{12})$, despite the lack of a slope change in the temperature dependence of the transverse frequency ν_T (see Fig. 6). This might be due to the fact that the L mode and the T mode of Fig. 6 are not purely longitudinal or transverse. Also, a small slope change in the ν_T plot might still be present, however then with an effect less than the experimental accuracy.

VI. CONCLUSION

The elastic properties of α -AgI have been obtained by Brillouin scattering from crystals of arbitrary grown orientations. The elastic constants were found to be small compared to normal low-conductivity ionic crystals, which seems to be an essential characteristic of a crystal to achieve high ionic conductivity. Contrary to neutron scattering observations, no damping of the transverse-acoustic modes could be observed. A structural change within the high-conductivity phase was revealed in the temperature range 620–700 K from measurements of the behavior of the longitudinal-acoustic mode. The effect supports a proposed cationic order-disorder transition in the observed temperature range. The obtained acoustic attenuation is attributed to a coupling between longitudinal phonons and a redistribution of the local Ag^+ population from equivalent to inequivalent sites, the obtained value being close to that predicted from theoretical considerations.

ACKNOWLEDGMENTS

This program is financially supported by the Swedish Natural Science Research Council. We gratefully acknowledge partial support from the Carl Tryggers and the Axel och Margaret Ax:son Johnssons Foundations.

¹*Topics of Current Physics 15, Superionic Conductors*, edited by M. B. Salamon (Springer, Berlin, 1979).

²K. Funke, in *Microscopic Structure and Dynamics of Liquids*, edited by J. Duprey and A. J. Dianoux (Plenum, New York, 1978).

³C. Tubandt and E. Lorentz, *Z. Phys.* **87**, 513 (1914).

⁴B. A. Huberman and R. M. Martin, *Phys. Rev. B* **13**, 1498 (1976).

⁵K. R. Subbaswamy, *Solid State Commun.* **19**, 1157 (1976); **21**, 371 (1977).

⁶P. Vashishta and A. Rahman, in *Fast Ion Transport in Solids*, edited by Vashishta, Mundy, and Shenoy (North-Holland, Amsterdam, 1979).

⁷R. Aronsson and L. M. Torell, following paper, *Phys. Rev. B* **36**, 4926 (1987).

⁸W. S. Gornall and B. P. Stoicheff, *Phys. Rev. B* **4**, 4518 (1971); S. Gewurtz and B. P. Stoicheff, *ibid.* **10**, 3487 (1974); **11**, 1705 (1975).

⁹L. W. Strock, *Z. Phys. B* **25**, 441 (1934); **31**, 132 (1936).

¹⁰S. Hoshino, T. Sakuma, and Y. Fujii, *Solid State Commun.* **22**, 763 (1977).

¹¹A. F. Wright and B. E. F. Fender, *J. Phys. C* **10**, 2261 (1977).

¹²J. B. Boyce, T. M. Hayes, and J. C. Mikkelsen, Jr., *Phys.*

Rev. B **23**, 2876 (1981).

¹³G. Burns, F. H. Dacol, and M. W. Shafer, *Phys. Rev. B* **16**, 1416 (1977).

¹⁴R. J. Cava, F. Reidinger, and B. J. Wuench, *Solid State Commun.* **24**, 441 (1977).

¹⁵A. Kvist and R. Tärneberg, *Z. Naturforsch. Teil A* **25**, 257 (1970).

¹⁶R. M. Martin, *Phys. Rev. B* **1**, 4005 (1970).

¹⁷T. A. Fjeldly and R. C. Hanson, *Phys. Rev. B* **10**, 3569 (1974).

¹⁸W. Bühner and P. Brüesch, *Solid State Commun.* **16**, 155 (1975).

¹⁹M. Bucher, *Phys. Rev. B* **30**, 947 (1984).

²⁰W. G. Kleppman, *J. Phys. C* **9**, 2285 (1976).

²¹B. Dorner, J. Windscheiff, and W. von der Osten, in *Lattice Dynamics*, edited by M. Balkanski (Flammarion, Paris, 1977).

²²R. T. Harley, W. Hayes, A. J. Rushworth, and J. F. Ryan, *J. Phys. C* **8**, L530 (1975).

²³C. R. A. Catlow, R. T. Harley, and W. Hayes in *Proceedings of the International Conference on Lattice Dynamics*, edited by M. Balkanski (Flammarion, Paris, 1977); *J. Phys. C* **10**, L559 (1977).

- ²⁴Cao-Xuan An, *Phys. Status Solidi A* **43**, K69 (1977).
- ²⁵G. Winterling, W. Senn, M. Grimsditch, and R. Katiyar, in *Proceedings of the International Conference on Lattice Dynamics*, Ref. 23.
- ²⁶W. Sasaki, Y. Sasaki, S. Ushioda, and W. Taylor, *J. Phys. Colloq.* **42**, C6-181 (1981).
- ²⁷R. Aronsson, L. Börjesson, and L. M. Torell, *Solid State Ionics* **8**, 147 (1983).
- ²⁸C. M. Perrot and N. H. Fletcher, *J. Chem. Phys.* **50**, 2770 (1969); **55**, 4681 (1971).
- ²⁹A. Fontana, G. Mariotto, and M. P. Fontana, *Phys. Rev. B* **21**, 1102 (1980).
- ³⁰G. Mariotto, A. Fontana, E. Cazzanelli, F. Rocca, M. P. Fontana, V. Mazzacurati, and G. Signorelli, *Phys. Rev. B* **23**, 4782 (1981); **26**, 2216 (1982).
- ³¹J. Tallon, *Phys. Rev. Lett.* **57**, 2427 (1986).
- ³²H. Goldstein, *Classical Mechanics* (Addison-Wesley, Cambridge, 1950), p. 107.
- ³³G. B. Benedek and K. Fritsch, *Phys. Rev.* **149**, 647 (1966).
- ³⁴J. Kowalik and M. R. Osborne, *Methods for Unconstrained Optimization Problems* (Elsevier, New York, 1968).
- ³⁵S. E. Gustavsson and E. Karawacki, *Appl. Optics* **14**, 1105 (1975); *Z. Naturforsch.* **319**, 956 (1976).
- ³⁶C. Kittel, *Introduction to Solid State Physics* (Wiley, New York, 1971).
- ³⁷L. Strock, *Z. Phys. B* **25**, 441 (1934).
- ³⁸J. Vallin, *Ark. Fys.* **34**, 367 (1967).
- ³⁹P. Brüesch, W. Bühler, and H. J. M. Smeets, *Phys. Rev. B* **22**, 970 (1980).
- ⁴⁰L. M. Torell, *Phys. Rev. B* **31**, 4103 (1985); L. Börjesson, S. W. Martin, L. M. Torell, and C. A. Angell, *Solid State Ionics* **18&19**, 431 (1986).
- ⁴¹H. B. Huntington, in *Solid State Physics*, edited by Seitz and Turnbull (Academic, New York, 1958), Vol. 7.
- ⁴²M. T. Sprackling, *Plastic Deformation of Simple Ionic Crystals* (Academic, London, 1976).